



City Research Online

City St George's, University of London

Citation: Gatheeshgar, P., Poologanathan, K., Gunalan, S., Shyha, I., Tsavdaridis, K. D. & Corradi, M. (2020). Optimal design of cold-formed steel lipped channel beams: Combined bending, shear, and web crippling. *Structures*, 28, pp. 825-836. doi: 10.1016/j.istruc.2020.09.027

This is the accepted version of the paper.

This version of the publication may differ from the final published version. To cite this item please consult the publisher's version.

Permanent repository link: <https://openaccess.city.ac.uk/id/eprint/27689/>

Link to published version: <https://doi.org/10.1016/j.istruc.2020.09.027>

Copyright and Reuse: Copyright and Moral Rights remain with the author(s) and/or copyright holders. Copies of full items can be used for personal research or study, educational, or not-for-profit purposes without prior permission or charge, unless otherwise indicated, provided that the authors, title and full bibliographic details are credited, a hyperlink and/or URL is given for the original metadata page and the content is not changed in any way. For full details of reuse please refer to [City Research Online policy](#).

Structures

Optimal Design of Cold-Formed Steel Lipped Channel Beams: Combined Bending, Shear, and Web Crippling

Perampalam Gatheeshgar

Faculty of Engineering and Environment, Northumbria University,
Newcastle upon Tyne, UK.

Keerthan Poologanathan

Faculty of Engineering and Environment, Northumbria University,
Newcastle upon Tyne, UK.

Shanmuganathan Gunalan

School of Engineering and Built Environment, Griffith University,
Gold Coast Campus, Australia.

Islam Shyha

Faculty of Engineering and Environment, Northumbria University
Newcastle upon Tyne, UK.

Konstantinos Daniel Tsaydaridis

School of Civil Engineering, Faculty of Engineering and Physical Sciences, University of Leeds,
Leeds, UK

Marco Corradi

Faculty of Engineering and Environment, Northumbria University
Newcastle upon Tyne, UK.

Abstract

The load carrying capacity of cold-formed steel (CFS) beams can be enhanced by employing optimisation techniques. Recent research studies have mainly focused on optimising the bending capacity of the CFS beams for a given amount of material. However, to the best of authors' knowledge, very limited research has been performed to optimise the CFS beams subject to shear and web crippling actions for a given amount of material. This paper presents the optimisation of CFS lipped channel beams for maximum bending, shear, and web crippling actions combined, leading to a novel conceptual development. The bending, shear and web crippling strengths of the sections were determined based on the provisions in Eurocode 3, while the optimisation process was performed by the means of Particle Swarm Optimisation (PSO) method. Combined theoretical and manufacturing constraints were imposed during the optimisation to ensure the practicality of optimised CFS beams. Non-linear Finite Element (FE) analysis with imperfections was employed to simulate the structural behaviour of optimised CFS lipped channel beams after successful validation against previous experimental results. The results demonstrated that, the optimised CFS sections are more effective (bending, shear,

Structures

37 and web crippling actions resulted in 30 %, 6 %, and 13 % of capacity increase, respectively)
38 compared to the conventional CFS sections with same amount of material (weight). The
39 proposed optimisation framework can be used to enhance the structural efficiency of CFS
40 lipped channel beams under combined bending, shear, and web crippling actions.

41 *Keywords:* Cold-Formed Steel Beams; Bending Strength; Shear Strength; Web Crippling
42 Strength; Combined Optimisation; Finite Element Analysis.

43 **1 Introduction**

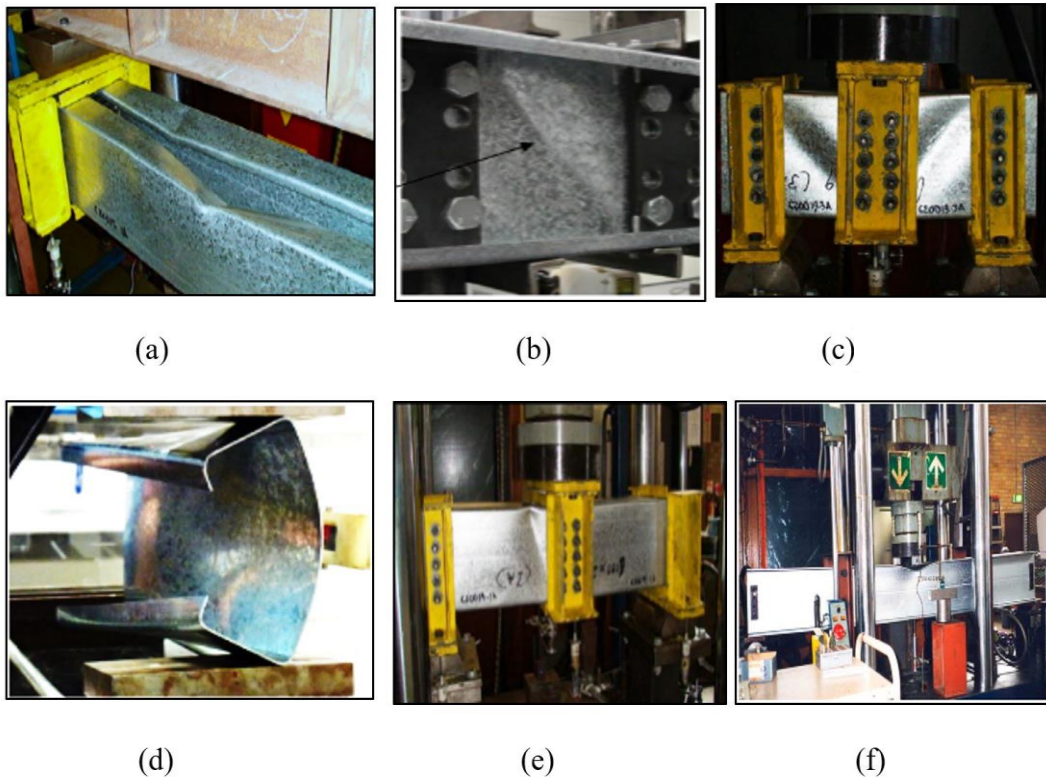
44 Cold-formed steel (CFS) members offer more economical and efficient design solutions as they
45 offer high strength-to-weight ratio, leading to material savings. Consequently, CFS members
46 have been widely employed in a broad range of civil and structural engineering applications.
47 The structural applications mainly include basic building elements for on-site assembly or
48 prefabricated floor and wall panels, as well as volumetric modular units. However, due to their
49 limited thickness, CFS members are highly prone to buckling instabilities. Prominent
50 consideration is, therefore, given during the design process.

51 CFS beams are used as primary and secondary load-bearing elements. They fail majorly in
52 bending, shear, web crippling or a combination of the above. Many research studies have
53 performed experimental works [1-5] and numerical studies [6-12] to examine the ultimate
54 cross-sectional resistance strength and behaviour of the CFS beams subject to the
55 aforementioned prominent and combined actions. In particular, Fig. 1 depicts all possible
56 failure modes of CFS beams. The sophisticated improvements in manufacturing technologies
57 along with the cross-sectional flexibility nature of CFS lead to necessitated modifications into
58 the CFS profiles.

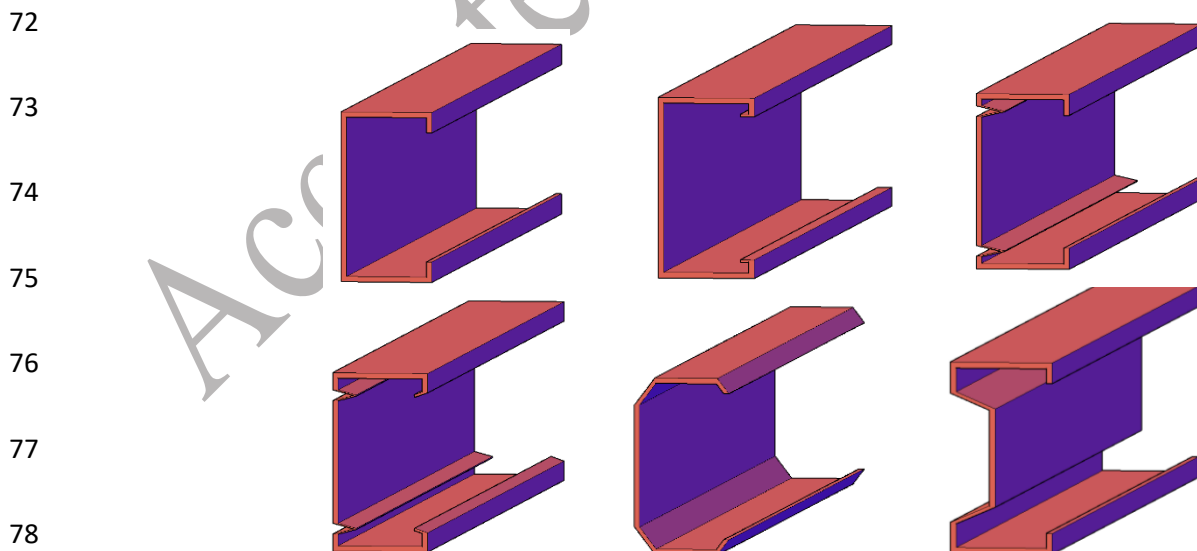
59 In recent years, optimisation techniques have also been employed to enhance the bending
60 performance of CFS beams. Such increased research focus resulted in novel CFS beam shapes
61 with enhanced bending capacities. For example, Ye et al. [13, 14] optimised the lipped channel
62 beams with intermediate web stiffeners and return lips, and introduced a novel folded-flange
63 section. Gatheeshgar et al. [15-17] performed optimisation studies of CFS sections and
64 introduced optimised super-sigma sections which can bear approximately 65% higher bending
65 capacity compared to the conventional lipped channel beam with the same amount of material.
66 They also investigated the relevant shear and web crippling capacities of the optimised sections
67 and found that the optimised novel sections performed poorly compared to the lipped channel

Structures

68 beam with the same amount of material. Fig. 2 shows the novel optimised sections considering
69 section moment capacity [13-16].



70 **Fig.1** Different types of failure modes of CFS beams: (a) bending [1]; (b,c) shear [5, 6]; (d) web crippling [4];
71 (e) combined bending and shear [6]; (f) combined bending and web crippling [7].



72
73
74
75
76
77
78
79 **Fig. 2** Optimised CFS beam sections for bending maintaining the same amount of material [13-16].

Structures

80 It is worth to note that there are circumstances where CFS beams can fail not only
81 predominantly in bending but also in shear, and web crippling actions. Shear failure is critical
82 in short spans while web crippling failure occurs when CFS beams subjected to concentrated
83 loads. Therefore, it is necessary to consider the shear and web crippling behaviour of the
84 sections during the optimisation process. This will ensure the optimised beams can also
85 perform efficiently under bending, shear, and web crippling, and thus they can be used in
86 specific building applications.

87 The objectives of this paper are to (a) optimise the CFS lipped channel beams for bending,
88 shear, and web crippling actions individually and (b) develop a novel concept of optimisation
89 procedure to produce a lipped channel beam which can comparatively perform well in all three
90 aforementioned actions. The optimisation was performed using Particle Swarm Optimisation
91 (PSO) method and the objective functions were developed using Eurocode 3 [18, 19]
92 guidelines. Finite Element (FE) models of lipped channel beams were developed and carefully
93 validated against the test results. The validated FE models were then used to simulate the
94 bending, shear, and web crippling strength and the combined behaviour of the optimised lipped
95 channel beams. Finally, the optimised sections were compared with a commercially available
96 lipped channel beam of the same amount of material (i.e., weight) to highlight any structural
97 benefits. The potential advantages of employing specific optimisation techniques are also
98 discussed via the analysed results and conclusions are drawn.

99 **2 Eurocode 3 design rules for lipped channel beams**

100 2.1 Bending

101 For the lipped channel beam, bending capacity was determined based on the effective width
102 method provisions adopted in EN1993-1-3 [18] and EN1993-1-5 [19]. Both local and
103 distortional buckling was taken into account in calculating the stiffness of the lipped channel
104 beams. The local buckling effects of the internal compression (web and flange), and outstand
105 compression (lip) elements were calculated based on the effective widths (compressive stress
106 concentration at the corners) as defined in EN1993-1-5 [19]. The local and distortional
107 buckling of a typical lipped channel beam is shown in Fig. 3. According to EN1993-1-5 [19]
108 the effective width of the internal and outstand compression elements for local buckling can be
109 calculated using a reduction factor on the plate width (ρ). Eqs. 1 and 2 provide the reduction
110 factor values for internal and outstand compression elements, respectively.

Structures

111

112

113

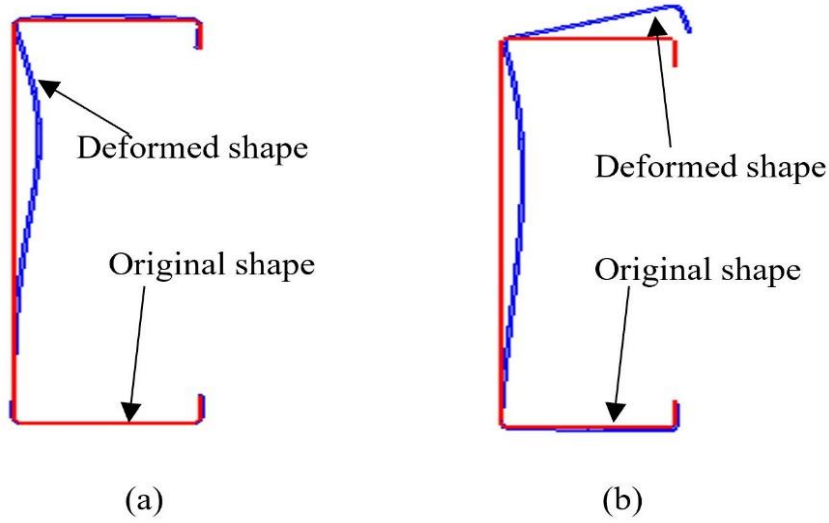
114

115

116

117

118



119

120

121

Fig. 3 Buckling types of a laterally braced CFS lipped channel beam subjected to bending stress: (a) local buckling; (b) distortional buckling.

122

$$\rho = \left[\frac{\lambda_p^{-0.055(3+\psi)}}{\lambda_p^2} \right] \quad (1)$$

123

$$\rho = \left[\frac{\lambda_p^{-0.188}}{\lambda_p^2} \right] \quad (2)$$

124

125

In Eqs. 1 and 2, ψ is the ratio of the end stress in the plate element and λ_p is the slenderness ratio ($= \sqrt{f_y/\sigma_{cr}}$; f_y = yield strength and σ_{cr} is the elastic critical plate buckling stress).

126

127

128

129

130

131

132

133

134

135

In contrast to the cross-sectional width concept for local buckling, the distortional buckling of the flange-lip juncture is taken into consideration through reducing the effective plate thickness. The distortional buckling effect in lipped channel beam is mainly governed by the elastic critical stress of the edge stiffener ($\sigma_{cr,s}$). This is calculated simulating the restraint provided by the adjacent plates into a spring stiffness (K) and determining the effective cross-section area (A_s) and second moment of area (I_s) of the edge stiffener. The corresponding Young's modulus of the material (E) also needs to be used (see Eq.3). The reduction factor for the distortional buckling (χ_d) is obtained from the slenderness ratio, and $\sigma_{cr,s}$ is to be used for this. The strength of the effective area of the stiffener is then reduced by χ_d . This aforementioned step needs to be repeated until the convergence of χ_d .

136

$$\sigma_{cr,s} = \frac{2\sqrt{KEI_s}}{A_s} \quad (3)$$

Structures

137 For the laterally braced beams, the ultimate bending capacity ($M_{c,Rd}$) is the minimum of the
138 bending capacity subject to local and distortional buckling failure.

139 2.2 Shear

140 The shear resistance capacity of the CFS lipped channel beams majorly depends on the web
141 buckling and the contribution from the flange is likely to be negligible [5]. According to
142 EN1993-1-5 [19] the design shear resistance ($V_{b,Rd}$) is given by the sum of web shear resistance
143 ($V_{bw,Rd}$) and flange shear resistance ($V_{bf,Rd}$), as given in Eq. 4. Eq. 5 provides the formula for
144 web shear resistance.

$$145 \quad V_{b,Rd} = V_{bw,Rd} + V_{bf,Rd} \leq \frac{\eta f_{yw} h_w t}{\sqrt{3} \gamma_{M1}} \quad (4)$$

$$146 \quad V_{bw,Rd} = \frac{\chi_w f_{yw} h_w t}{\sqrt{3} \gamma_{M1}} \quad (5)$$

147 where f_{yw} is the yield stress of the web, h_w is the clear web depth between the flanges and t is
148 the thickness of the plate. EN1993-1-5 [19] recommends the value of 1.20 for η up to the steel
149 grade S460 and value of 1.0 for higher steel grades. γ_{M1} is the partial factor. χ_w is the shear
150 buckling reduction factor for the web. The web was assumed to be a rigid end post condition
151 when calculating the shear buckling reduction factor of the web, χ_w . Moreover, the condition
152 of transverse web stiffeners at supports and intermediate span was considered to determine the
153 slenderness ratio (λ_w). The equation for the slenderness ratio is as follows:

$$154 \quad \lambda_w = \frac{h_w}{37.4 t \varepsilon \sqrt{k_\tau}} \quad (6)$$

155 Where ε and k_τ denote the factor depending on f_{yw} and minimum shear buckling coefficient
156 of the web panel, respectively. Annex A of EN1993-1-5 [19] carries the equations (see Eqs. 7
157 and 8) for the shear buckling coefficient (k_τ) of plates with rigid transverse stiffeners and
158 without longitudinal stiffeners in terms of the distance between transverse stiffeners (a) and
159 clear web depth between the flanges (h_w).

$$160 \quad k_\tau = 5.34 + \frac{4.00}{(a/h_w)^2} \quad \text{for } \frac{a}{h_w} \geq 1 \quad (7)$$

$$161 \quad k_\tau = 4.00 + \frac{5.34}{(a/h_w)^2} \quad \text{for } \frac{a}{h_w} < 1 \quad (8)$$

162 Even though provisions for the contribution from the flange on shear capacity are given in
163 EN1993-1-5 [19], they were not considered in this study as the flange contributes a relatively
164 small proportion to the total shear resistance [5, 20]. Their investigations showed that for most

Structures

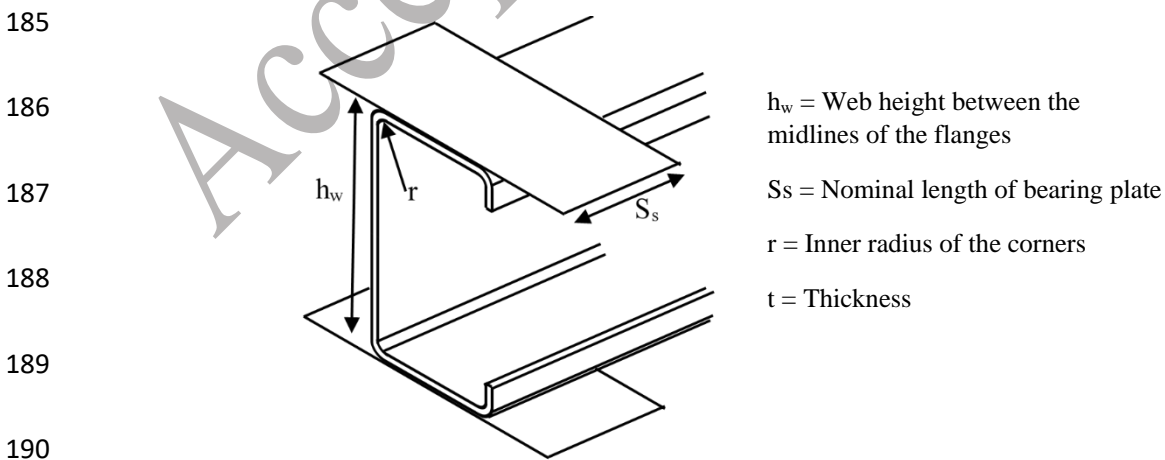
165 of the lipped channel sections the condition to consider the contribution to the shear capacity
166 from flange cannot be met and for the sections which meet the condition, the calculated shear
167 contribution from flange is negligible.

168 2.3 Web crippling

169 Web crippling failure occurs when CFS beams are subjected to concentrated loads. EN1993-
170 1-3 [18] categorises the web crippling failure of the cross-sections with single web into four
171 groups depending on the load cases: End-Two-Flange (ETF), Interior-Two-Flange (ITF), End-
172 One-Flange (EOF), and Interior-One-Flange (IOF). However, only the ETF load case was
173 considered in this study. Because for a typical section with a lower thickness, web crippling
174 strength is lower for ETF load case compared to other load cases based on EN1993-1-3 [18]
175 calculations. Eq. 9 presents the web crippling strength ($R_{w,Rd}$) as given in EN1993-1-3 [18].
176 This equation is valid for the cross-sections that comply with $r/t \leq 6$ (r =internal radius) and h_w/t
177 ≤ 200 conditions.

$$178 \quad R_{w,Rd} = \frac{k_1 k_2 k_3 \left[6.66 - \frac{h_w/t}{64} \right] \left[1 + 0.01 \frac{S_s}{t} \right] t^2 f_y}{\gamma_{M1}} \quad (9)$$

179 Where the values of the coefficient are determined such that $k_1 = 1.33 - 0.33k$ where $k = f_y/228$,
180 $k_2 = 1.15 - 0.15(r/t)$ but $0.5 \leq k_2 \leq 1.0$, and $k_3 = 1$ for lipped channel beams. S_s is the nominal length
181 of the bearing plate. A graphical illustration for the cross-sectional dimensions is depicted in
182 Fig.4. It is worth to note that EN1993-1-3 [18] carries no separate equations for fastened and
183 unfastened situations for ETF load case. Therefore, as a conservative approach, the flanges
184 unfastened condition was considered in this study.



191 **Fig. 4** Graphical illustration of the cross-sectional dimensions for ETF load case web crippling

Structures

192 3 Optimisation procedure for bending, shear, and web crippling

193 3.1 General

194 This section provides details on the formulation of the optimisation problem under different
195 conditions and implemented practical and manufacturing constraints. Optimisation is
196 nowadays an important approach to obtain economical designs with enhanced structural
197 efficiency. The PSO algorithm was used to perform the optimisation while the cross-section
198 resistant capacity design equations discussed in section 2 were used as objective functions.
199 Extensive detail on the description of PSO optimisation can be found in the literature [13-16].
200 A commercially available lipped channel beam was set as a reference section (see Fig. 5). This
201 section has a total coil length of 415 mm and thickness of 1.5 mm. The yield strength, Young's
202 modulus, and Poisson's ratio of the reference section are 450 MPa, 210 GPa, and 0.3,
203 respectively. Similar cross-sectional (coil length and thickness) and mechanical properties
204 (yield strength, Young's modulus, and Poisson's ratio) were adopted in the optimisation
205 process to assess the degree of improvement of the optimised sections for a given amount of
206 material used.

207

208

209

210

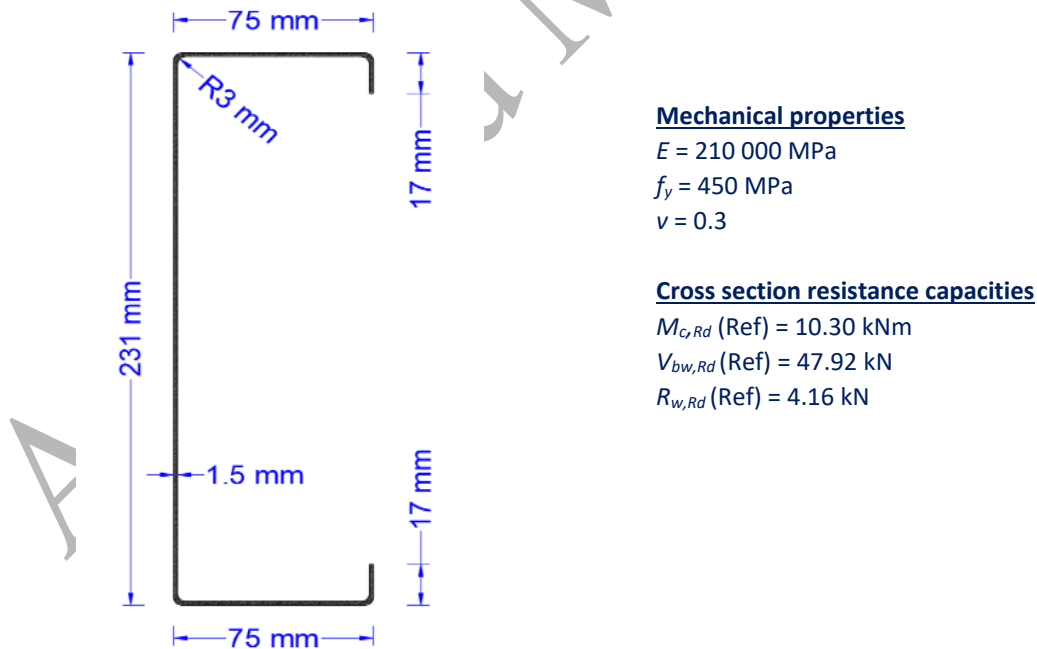
211

212

213

214

215



216

Fig. 5 Dimensions, mechanical properties, and cross-section resistance capacities of the reference section.

Structures

217 3.2 Optimisation formulation for bending

218 As discussed in section 2.1, the bending failure of a CFS beam can occur subject to local and
219 distortional buckling failures, assuming that beam is laterally braced. The objective function is
220 formulated such that considering the minimum of local and distortional buckling capacities.
221 The flange (b), web (h) and lip (c) length were considered as design variables during the
222 optimisation for bending. The objective function for bending is defined by:

$$223 \quad \text{Maximize } [M_{c,Rd}(x)] = W_{eff}(x) \cdot f_y / \gamma_{M1} \quad (10)$$

224 Where $M_{c,Rd}(x)$ is the section moment capacity of the lipped channel beam for each design
225 variable. $W_{eff}(x)$ is the section modulus of the lipped channel section. These variables were set
226 to vary within the theoretical and manufacturing constraints.

227 3.3 Optimisation formulation for shear

228 To formulate the objective function to determine the shear capacity of the lipped channel
229 beams, Eq. 5 was used. During the optimisation, only the web height was considered as design
230 variable as the contribution from the flange is negligible, as explained in section 2.2. The
231 objective function to optimise the shear capacity is defined by:

$$232 \quad \text{Maximize } [V_{bw,Rd}(x)] = \frac{\chi_w(x) f_{yw} h_w(x) t}{\sqrt{3} \gamma_{M1}} \quad (11)$$

233 Where all the variables are defined similar in section 2.2.

234 3.4 Optimisation formulation for web crippling

235 Similar to shear behaviour, according to the provisions provided in Eurocode 3 [18, 19], the
236 web crippling strength of the lipped channel beam is also mainly governed by the web.
237 Therefore, only the dimension of the web was considered as variable during the optimisation.
238 The considered objective function for the optimisation is given in Eq. 12.

$$239 \quad \text{Maximize } [R_{w,Rd}(x)] = \frac{k_1 k_2 k_3 \left[6.66 - \frac{h_w(x)/t}{64} \right] \left[1 + 0.01 \frac{S_s}{t} \right] t^2 f_y}{\gamma_{M1}} \quad (12)$$

240 Where all the variables are defined as similar in section 2.3 and Fig 4. A value of 100 mm was
241 selected for the length of the bearing plate, S_s . This length was selected to avoid the flange

Structures

242 crushing behaviour which has substantial influence in the web crippling capacity for low value
243 of S_s [8].

244 3.5 Optimisation formulation for overall/combined performance

245 The concept of combined optimisation of lipped channel beam is necessary to enhance the
246 overall performance of the cross-section. Lee et al. [21] developed an optimum design
247 procedure using micro genetic algorithm for simply supported CFS beams subjected to
248 uniformly distributed loads. They aimed to reduce the weight of the CFS beam section subject
249 to defined magnitude of distributed load to satisfy the bending, shear, web crippling, and
250 deflection criteria. However, the optimisation was performed for un-lipped channels.
251 Therefore, this study intends to develop a combined optimisation methodology under ultimate
252 limit state conditions for lipped channel beams. The general design procedure for a lipped
253 channel beam includes bending, shear, and web crippling failure considerations. The aim is to
254 develop an optimised section with a maximised capacity which can over-perform under all
255 bending, shear, and web crippling actions compared to the reference section (depicted in Fig.
256 5) while having the same amount of material. Therefore, all the objective functions developed
257 in section 3.1, 3.2, and 3.2 were combined to produce a unified objective function. The web,
258 flange, and lip dimensions were considered as the design variables. Eq. 13 represents the
259 developed unified objective function for combined optimisation.

$$260 \quad \text{Max } [MVR(x)] = \left(\frac{M_{c,Rd}(x)}{M_{c,Rd(Ref)}} \right) + \left(\frac{V_{bw,Rd}(x)}{V_{b,Rd(Ref)}} \right) + \left(\frac{R_{w,Rd}(x)}{R_{w,Rd(Ref)}} \right) \quad (13)$$

$$261 \quad \text{Subjected to:} \quad \left(\frac{M_{c,Rd}(x)}{M_{c,Rd(Ref)}} \right) \geq 1.0$$

$$262 \quad \left(\frac{V_{bw,Rd}(x)}{V_{b,Rd(Ref)}} \right) \geq 1.0$$

$$263 \quad \left(\frac{R_{w,Rd}(x)}{R_{w,Rd(Ref)}} \right) \geq 1.0$$

264 Eq. 13 has been developed adding three ratios pertaining to bending, shear, and web crippling.
265 These are the ratios between the relevant capacity of optimised sections and relevant capacity
266 of the reference section (Fig. 4) for bending, shear, and web crippling, accordingly. Each ratio
267 was set to be greater than 1.0 in order to obtain the optimum lipped channel section with higher
268 capacities compared to the reference lipped channel section. This combined optimisation
269 resulted in promising results, as none of the capacities was reduced compared to their

Structures

270 corresponding reference lipped channel beam capacities. Table 1 and Fig. 6 present the
 271 optimised capacities of the lipped channel beams with the same amount of material for bending,
 272 shear, web crippling and combined actions and the corresponding optimised dimensions,
 273 respectively. The performance of optimised lipped channel beams is illustrated in Fig. 7.

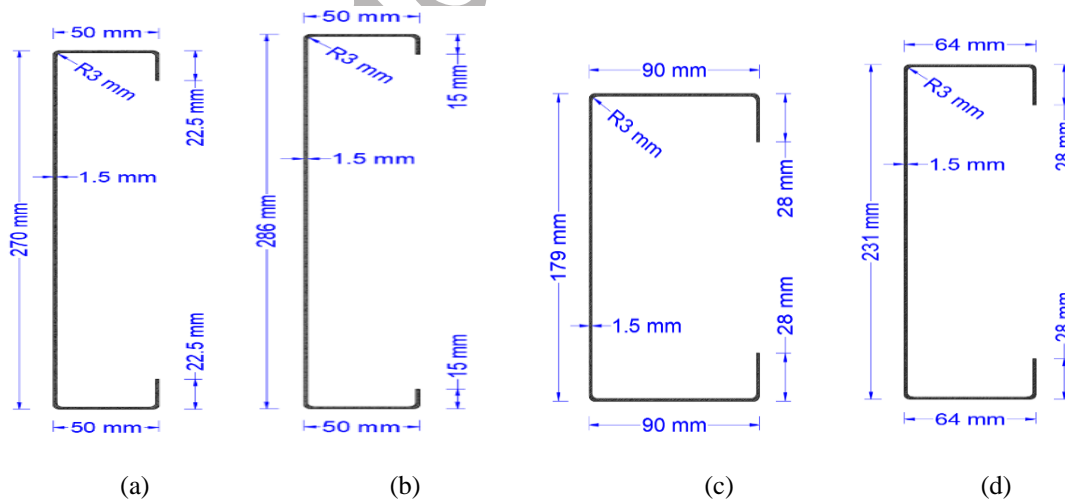
274

275 Table 1: Results of the optimised bending capacities for bending, shear, and combined performance (Capacities
 276 based on Eurocode3)

Actions interested in optimisation	Optimised capacities and other capacities			Reference and optimised dimensions			Performance factor			
	$M_{c,Rd}$ (kNm)	$V_{b,Rd}$ (kN)	$R_{w,Rd}$ (kN)	Web (mm)	Flange (mm)	Lip (mm)	$M_{c,Rd}/M_{c,Rd(Ref)}$	$V_{b,Rd}/V_{b,Rd(Ref)}$	$R_{w,Rd}/R_{w,Rd(Ref)}$	Total (Eq.13)
Reference (Fig. 5)	10.30	47.92	4.16	231	75	17	1.00	1.00	1.00	3.00
Bending (Eq. 10)	13.38	49.96	3.75	270	50	22.5	1.30	1.04	0.90	3.24
Shear (Eq. 11)	12.51	50.63	3.59	286	50	15	1.21	1.06	0.86	3.13
Web crippling (Eq. 12)	8.62	44.33	4.68	179	90	28	0.84	0.93	1.13	2.90
Combined (Eq. 13)	11.59	47.92	4.16	231	64	28	1.12	1.00	1.00	3.12

277 Note: $M_{c,Rd}$ = Section moment capacity, $V_{b,Rd}$ = Shear resistance, $R_{w,Rd}$ = Web crippling strength, $M_{c,Rd(Ref)}$ = Section
 278 moment capacity of reference section, $V_{b,Rd(Ref)}$ = Shear resistance of reference section, $R_{w,Rd(Ref)}$ = Web crippling strength
 279 of reference section.

280

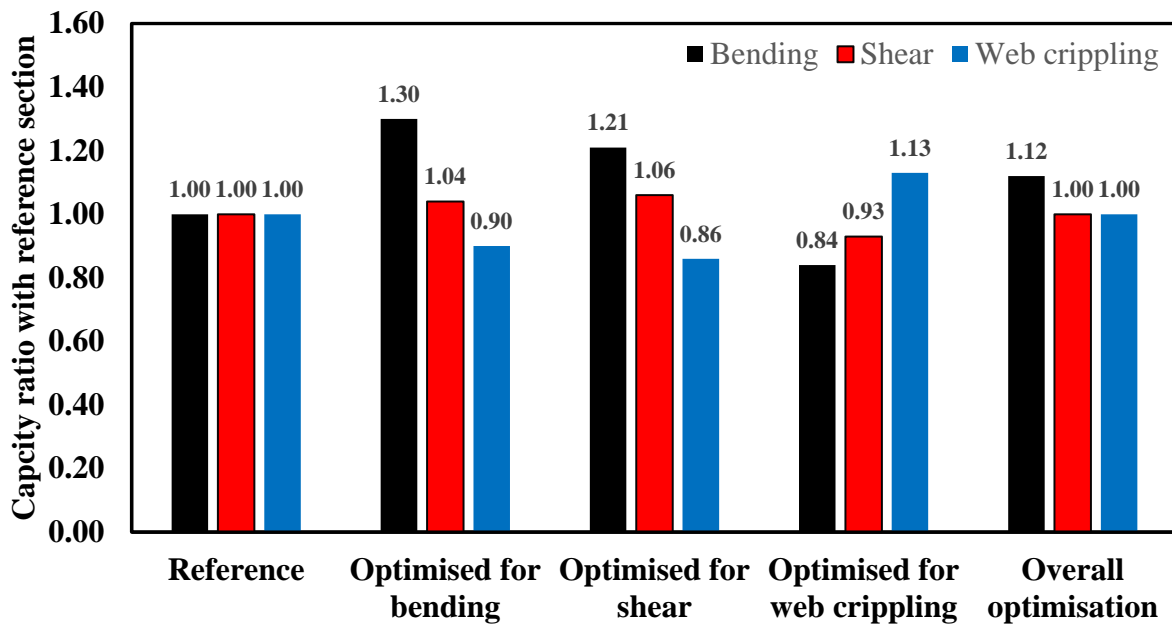


281

282

283 **Fig. 6** Dimensions of the optimised lipped channel beams under given constraints for considering individual and
 284 overall behaviour: (a) bending; (b) shear; (c) web crippling; (d) combined.

Structures



285

286

Fig. 7 Performance of optimised lipped channel beams

287 3.6 Imposed theoretical and manufacturing constraints

288 Theoretical and manufacturing constraints guide the optimisation to ensure the practicality of
 289 the resultant (optimum) dimensions of the lipped channel beams. The constraints for the
 290 optimisation were set in line with Eurocode 3 [18, 19] and current construction practices.
 291 EN1993-1-3 [18] states the following dimensional constraints for CFS beams: $b/t \leq 60$, $c/t \leq$
 292 50 , $0.2 \leq c/t \leq 0.6$, and $h/t \leq 500$ in usual notations. These constraints were fed into the
 293 optimisation problem. Regarding the practical and manufacturing constraints and in order to
 294 find out the bounds of the segments of lipped channel beams, a survey was conducted with
 295 help from an industrial partner to assess the dimensional limitations of the commercially
 296 available lipped channel beams. In total 530 lipped channel profiles from 17 different
 297 manufacturers across the UK were analysed and the range of the dimensional and mechanical
 298 values was mapped. Table 2 presents the findings of the survey on commercially available
 299 lipped channel beams. Combining the dimensional bounds obtained from the survey alongside
 300 with manufacturing constraints reported by Ye et al. [13], additional constraints were imposed.
 301 Even though the flange dimensions vary in between 34 mm and 125 mm, the lower bound was
 302 set to 50 mm to ensure the proper connection of the joist with floorboards and trapezoidal
 303 decking [13]. While the upper bound was set in line with Eurocode 3 [18, 19] limit. For the lip,
 304 the lower and upper bounds were selected as 15mm [13] and 28 mm, respectively. The length
 305 of the web was decided based on the coil length, web, and flange length. However, the height

Structures

306 of the web was limited to 300 mm and the minimum height of the web was set to 100 mm in
307 order to ensure connection plates can be fixed.

308 Table 2: Dimensional and yield strength bounds of commercially available lipped channel beams.

Profile parameters	Range
Web (mm)	60 – 500
Flange (mm)	34 – 125
Lip (mm)	7 – 28
Radius (mm)	0.9 – 8
Thickness (mm)	0.6 – 5
Coil length (mm)	154 – 750
Yield strength (MPa)	320 – 550

309

310 4 FE analysis and results

311 4.1 FE model

312 The bending, shear, and web crippling capacities of the reference and optimised lipped channel
313 beams were also obtained using a commercially available FE software, ABAQUS version 2017
314 [22]. FE analysis was aimed to verify the proposed optimisation approach and to investigate
315 the pre-buckling and post-buckling behaviours of the optimised lipped channel beams. For
316 bending and shear, the whole analysis procedure included two phases: eigenvalue buckling
317 analysis and non-linear analysis. For bending and shear models, initial geometric imperfections
318 were applied to the critical buckling mode (the lowest) obtained from the linear buckling
319 analysis while the imperfection magnitude was chosen according to Schafer and Pekoz [23].
320 For web crippling models, it was found that the effect of imperfection on web crippling strength
321 was negligible. Therefore, imperfections were not incorporated into the FE models.
322 Sundararajah et al.'s [8] finding also demonstrated that the effect of imperfection on web
323 crippling capacity is negligible (<1%) for two flange load cases.

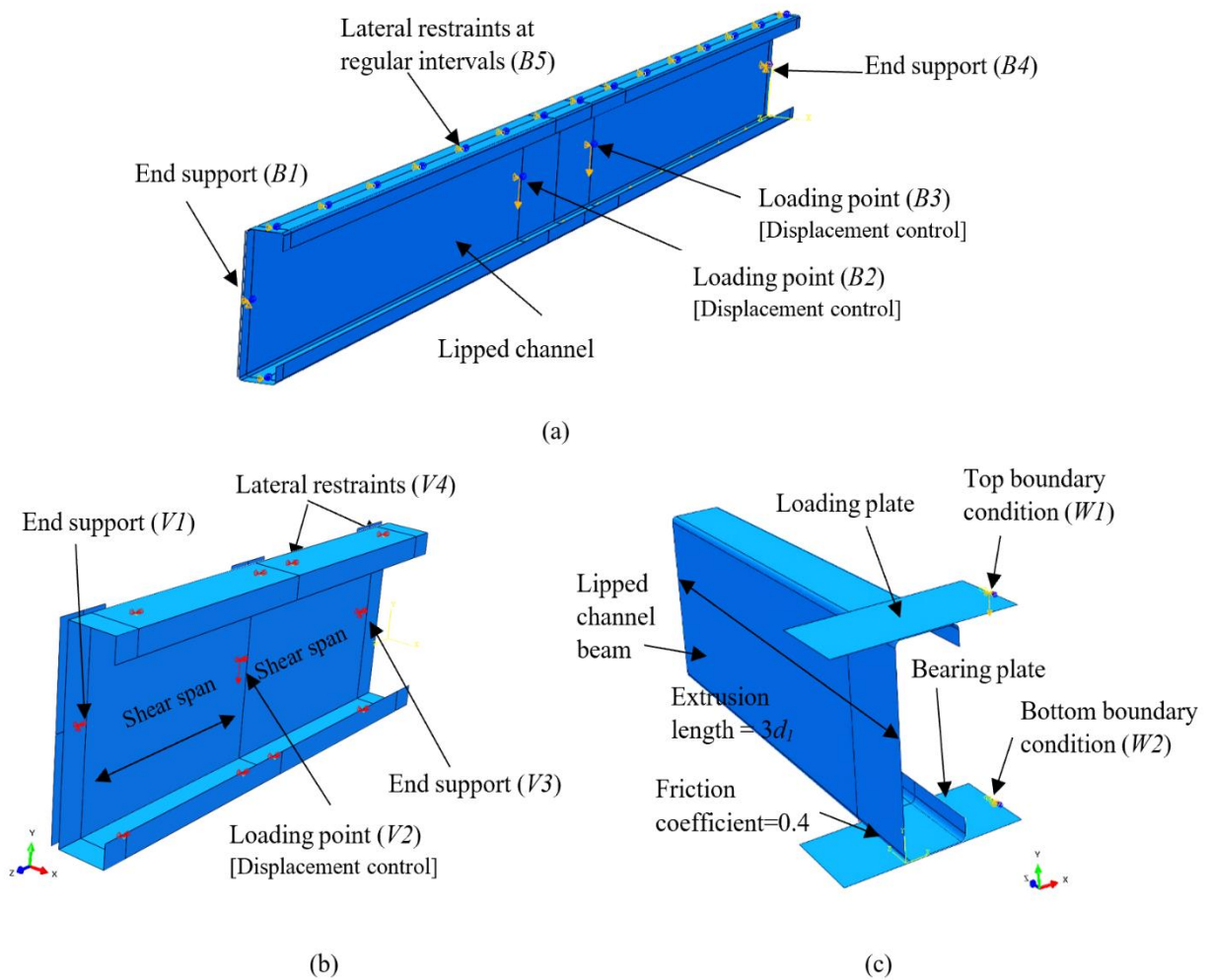
324 A four-point bending arrangement was used for the bending tests. This set-up ensures the pure
325 bending failure of the lipped channel beam at the mid-span with the absence of the shear force.
326 Three-point bending set-up was used to simulate the lipped channel beam subject to shear.
327 Herein, prominent shear failure was ensured by selecting the aspect ratio (=shear span/clear
328 web depth) equal to unity. However, to develop the web crippling FE model under ETF load
329 case, extrusion length of $3d_l$ [4], where d_l denotes the length of the flat portion of the web, was

Structures

330 used. Fig. 8 shows the schematic diagram of the FE models constructed in ABAQUS for
331 bending, shear, and web crippling, while Table 3 presents the adopted boundary conditions.
332 The load was applied in terms of displacement control at the loading points, while simply
333 supported boundary conditions were adopted. In bending models, lateral restraints were
334 provided at regular intervals (at top and bottom flanges) to restrain the lateral-torsional
335 buckling of the lipped channel beams, while in shear models, straps were simulated as
336 boundary conditions in flanges adjacent to the web side plates. The web side plates, in bending
337 and shear models, were connected using the 'tie' constraint option available in ABAQUS. On
338 the other hand, in web crippling models, bearing plates were connected using the 'hard' contact
339 alongside with the input of friction coefficient 0.4.

340 Material modelling is a key parameter. Haidarali and Nethcot [10] investigated four different
341 material models to identify the suitable stress-strain relationship for FE modelling. They
342 concluded that CFS material exhibits negligible strain hardening while the gradual yielding of
343 the material is essential in FE modelling. Siahaan et al. [24], Keerthan and Mahendran [25],
344 and Sundararajah et al. [8] successfully employed a bi-linear stress-strain curve with nominal
345 yield point and no strain hardening in the FE modelling of CFS beams subject to bending,
346 shear, and web crippling. Therefore, the stress-strain behaviour of the CFS beam was assumed
347 to be with an elastic-perfect plastic model with nominal yield-stress considering the negligible
348 strain-hardening in CFS. It is worth to mention that the effect of the residual stresses and corner
349 strength enhancement were not inputted into the FE models as both can approximately counter
350 affect each other [26].

Structures



351 **Fig. 8** Schematic diagram of the developed FE models with boundary conditions: (a) bending; (b) shear; (c) web
352 crippling.

353 A quadrilateral shell element with reduced integration, aka S4R in ABAQUS element library,
354 was employed for all analyses. Fig. 9 depicts the element types and mesh sizes of the FE
355 models. The lipped channel beams were refined with $5\text{ mm} \times 5\text{ mm}$ mesh size. Finer mesh size
356 ($1\text{ mm} \times 5\text{ mm}$) was used in corner regions. The web side plates (in bending and shear models)
357 and bearing plates (in web crippling model), which are used to provide the boundary conditions
358 and apply the load, were meshed with $10\text{ mm} \times 10\text{ mm}$ element size. In addition, bearing plates
359 were modelled using R3D4 rigid plate elements. These type of element types and mesh sizes
360 were successfully used in past research studies on FE modelling of CFS beams [6, 8, 9, 13, 15,
361 16, 27, 28]. The selected mesh sizes showed a good agreement with test results during the
362 validation process.

363

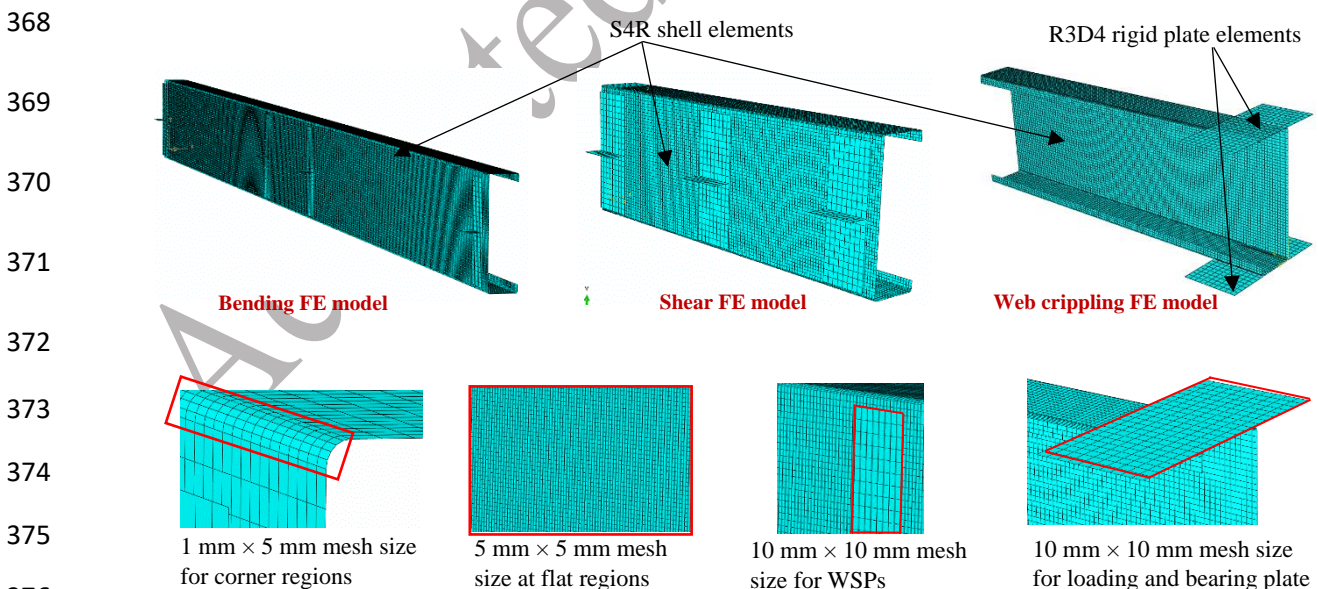
364

Structures

365 Table 3: Adopted boundary conditions in FE models

Locations marked in Fig.8	Boundary conditions					
	Translations			Rotations		
	UT_x	UT_y	UT_z	UR_x	UR_y	UR_z
Bending						
<i>B1</i>	Restrained	Restrained	Restrained	Free	Free	Restrained
<i>B2</i>	Restrained	Free	Free	Free	Free	Restrained
<i>B3</i>	Restrained	Free	Free	Free	Free	Restrained
<i>B4</i>	Restrained	Restrained	Free	Free	Free	Restrained
<i>B5</i>	Restrained	Free	Free	Free	Free	Restrained
Shear						
<i>V1</i>	Restrained	Restrained	Restrained	Free	Free	Restrained
<i>V2</i>	Restrained	Free	Free	Free	Free	Restrained
<i>V3</i>	Restrained	Restrained	Free	Free	Free	Restrained
<i>V4</i>	Restrained	Free	Free	Free	Free	Restrained
Web crippling						
<i>W1</i>	Restrained	Free	Restrained	Free	Free	Restrained
<i>W2</i>	Restrained	Restrained	Restrained	Free	Free	Restrained

366 Note: UT_x = Translation in x-direction, UT_y = Translation in y-direction, UT_z = Translation in z-direction, UR_x = Rotation
 367 about x-axis, UR_y = Rotation about y-axis, UR_z = Rotation about z-axis



377 **Fig. 9** Meshing outline and element types in FE models.

378

Structures

379 4.2 Validation of FE models

380 The aforementioned modelling characteristics were validated against the experimental results
 381 to ensure their capabilities in predicting accurately the cross-section resistance and behaviour.
 382 Pham and Hancock [1], Keerthan and Mahendran [5], and Sundararajah et al. [4] investigated
 383 the structural behaviour of the lipped channel beams subject to bending, shear and, web
 384 crippling through experimental studies. Six test results from each study were selected and
 385 validated against the FE results. Table 4 presents the comparison of ultimate moment capacities
 386 obtained from the FE analyses and test results. Section moment capacities obtained from FE
 387 analyses showed a good agreement with experiment bending test results with a mean value of
 388 0.97 and a Coefficient of Variation (COV) value of 0.07. Further, the comparison between the
 389 shear resisting capacities obtained from FE analyses and Keerthan and Mahendran's [5] test
 390 results is presented in Table 5. The shear resisting capacity ratios of FE models and test results
 391 registered in a good agreement with a mean and a COV values of 0.99 and 0.08, respectively.
 392 The six web crippling test results for the ETF load case with 100 mm bearing plate was selected
 393 for the web crippling validation as in the optimisation procedure; similar bearing plate length
 394 was also selected. Table 6 compares the web crippling capacity generated from FE models and
 395 tests results. From the scatter of results (COV=0.05) and a mean value of 0.93, it can be
 396 concluded that FE models are capable of predicting web crippling strength.

397

398 Table 4: Comparison of experimental and FE section moment capacities

LCB specimen	h (mm)	b (mm)	c (mm)	r (mm)	t (mm)	f_y (MPa)	Test [1] (kNm)	FE (kNm)	Test/FE
Mw_C15015	152.70	64.77	16.57	5.00	1.50	514.10	9.5	9.6	0.99
Mw_C15019	153.38	64.47	16.00	5.00	1.90	534.50	12.9	13.6	0.95
Mw_C15024	152.60	62.70	19.70	5.00	2.40	485.30	17.7	16.6	1.08
Mw_C20015	203.70	76.08	16.42	5.00	1.50	513.40	12.2	13.3	0.92
Mw_C20019	202.60	77.92	17.28	5.00	1.90	510.50	18.9	21.3	0.89
Mw_C20024	202.35	76.61	20.38	5.00	2.40	483.50	27.8	27.6	1.01
Mean									0.97
COV									0.07

399 Note: h = Web depth, b = Flange width, c = Lip length, r = Corner inner radius, t = Thickness, f_y = Yield strength

400

401

402

403

Structures

404 Table 5: Comparison of experimental and FE shear resistance capacities

LCB specimen	a/d ₁	d ₁ (mm)	t (mm)	f _y (MPa)	Test [5] (kN)	FE (kN)	Test/FE
160×65×15×1.90	1.0	156.8	1.92	515	73.8	77.58	0.95
200×75×15×1.50	1.0	197.0	1.51	537	57.0	61.90	0.92
160×65×15×1.50	1.0	157.5	1.51	537	54.5	55.20	0.99
120×50×18×1.50	1.0	116.8	1.49	537	43.3	47.80	0.91
200×75×15×1.95	1.0	198.0	1.93	271	55.1	50.07	1.10
120×50×18×1.95	1.0	118.6	1.95	271	38.1	34.88	1.10
Mean							0.99
COV							0.08

405 Note: a = Shear span, d₁ = Clear web depth, t = Thickness, f_y = Yield strength

406 Table 6: Comparison of experimental and FE web crippling strength under ETF load case

LCB specimen	l _b (mm)	f _y (mm)	t (mm)	r (mm)	t (mm)	b (mm)	c (mm)	h (MPa)	L (mm)	Test [4] (kN)	FE (kN)	Test/ FE
C10010	100	581	1.03	3.50	1.50	50.2	14	99.8	306	2.13	2.43	0.88
C10015	100	540	1.52	4.00	1.90	50.9	15.3	100.4	306	5.27	5.58	0.94
C15012	100	556	1.21	4.00	2.40	61.9	19.6	150.9	456	2.46	2.56	0.96
C15015	100	531	1.52	4.50	1.50	60	19.8	150	456	4.03	4.18	0.96
C20019	100	506	1.91	5.00	1.90	76.5	22	203.4	606	6.01	6.12	0.98
C20024	100	526	2.41	5.00	2.40	76.4	20.4	203.5	609	9.45	10.72	0.88
Mean												0.93
COV												0.05

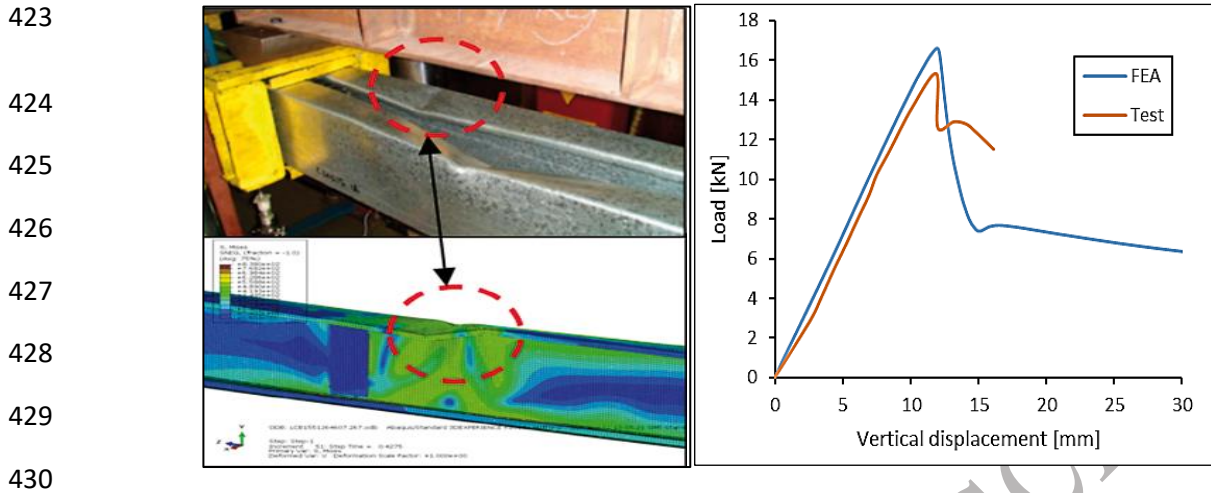
407 Note: l_b = Bearing plate length, f_y = Yield strength, t = Thickness, r = Corner inner radius, b = Flange width, c = Lip length,
408 h = Web depth, L = Specimen length.

409

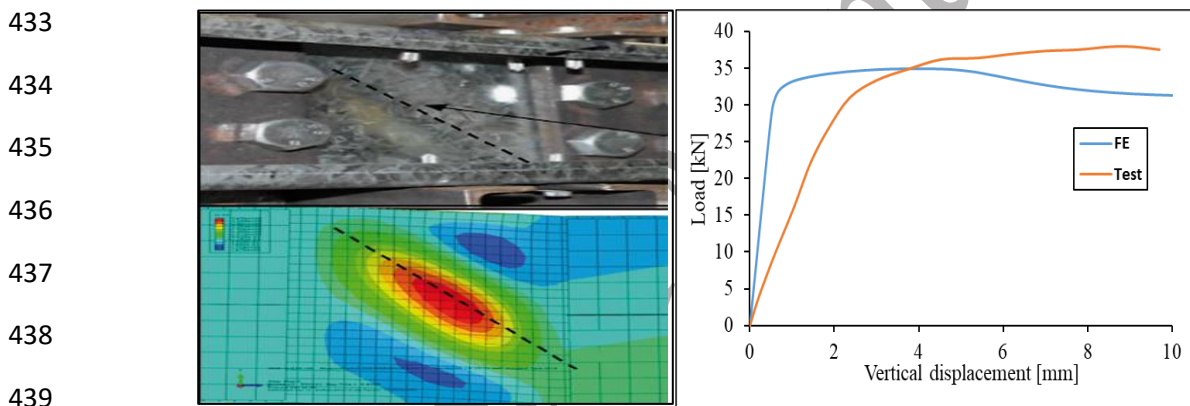
410 Figs. 10-12 show the moment/force-displacement responses and failure mode comparisons for
411 bending, shear, and web crippling, respectively. In Fig. 11, initial displacements obtained from
412 FE analysis are associated with lower displacements in comparison to laboratory test curve.
413 This is because the initial bolt slip which commonly occurs in laboratory tests. This is difficult
414 to simulate in FE modelling. Similar variation in force-displacement behaviour between test
415 and FE analysis has also been obtained by Pham and Hancock [6]. The trend of force-
416 displacement responses and failure modes obtained from the FE models correlate reasonably
417 well with the experimental results. Thus, pre-collapse, collapse, and post-collapse mechanisms
418 can be well-approximated through developed FE models. This ensures the accuracy of the FE
419 models predicting the cross-section resistance capacities. Therefore, the adopted FE model
420 characteristics produced a satisfactory agreement with experiment results, in terms of ultimate

Structures

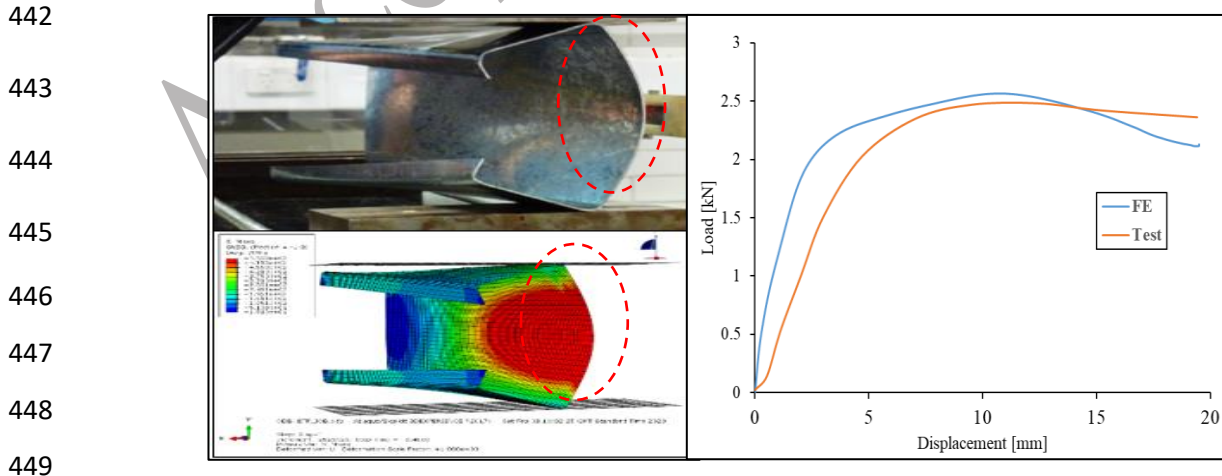
421 cross-sectional resistance capacity prediction, force-displacement response, and failure mode
422 comparison.



431 **Fig. 10** Comparison of experimental [1] and FE bending failure modes and force-displacement behaviour for
432 Mw_C20015 specimen



440 **Fig. 11** Comparison of experimental [5] and FE shear failure modes and force-displacement behaviour for
441 120x50x18x1.95 specimen



450 **Fig. 12** Comparison of experimental [4] and FE web crippling failure modes and force-displacement behaviour for
451 C15012 specimen

Structures

4.3 FE results

The validated FE models were then used to predict the strength and behaviour of the optimised lipped channel beams. Fig. 13 shows the stage-by-stage failure mode obtained from FE analysis for the optimised lipped channel beams for bending and its corresponding moment – displacement behaviour. Similarly, stage-by-stage failure modes obtained for the optimised lipped channel beams for shear and web crippling are illustrated in Fig. 14 and Fig. 15, respectively. The failure modes have shown a good illustration of the failure mechanism; failure at the compression flange for bending, diagonal failure for shear, and web buckling for web crippling. Moreover, the proposed optimisation approach can be verified by this FE analysis using the optimised sections. For that, the cross-sectional resistance capacities obtained from FE analyses were compared against the results obtained from Eurocode 3 (presented in Table 1). Table 7 presents the cross-sectional resistance capacities obtained from FE analyses for the optimised dimensions of lipped channel beams. The computational cross-section resistance capacities show a reasonable agreement with Eurocode 3 [18, 19] results except for the case for web crippling. Fig. 16 depicts the performance of the optimised lipped channel beams based on the FE results.

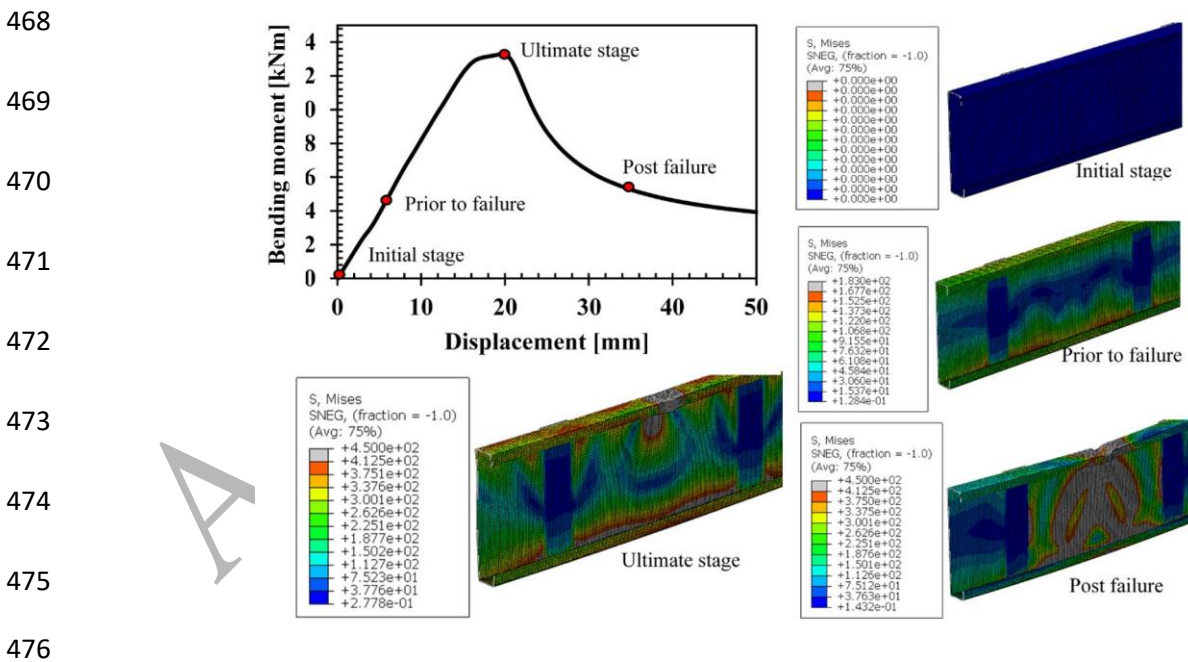
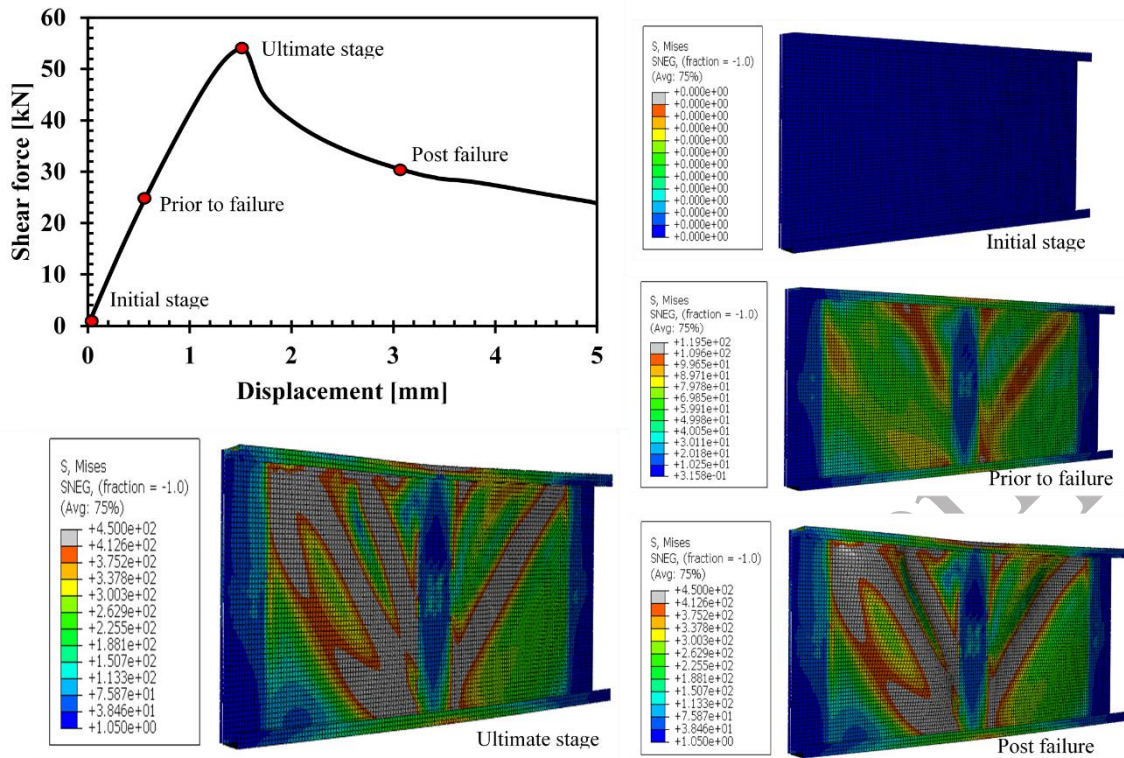


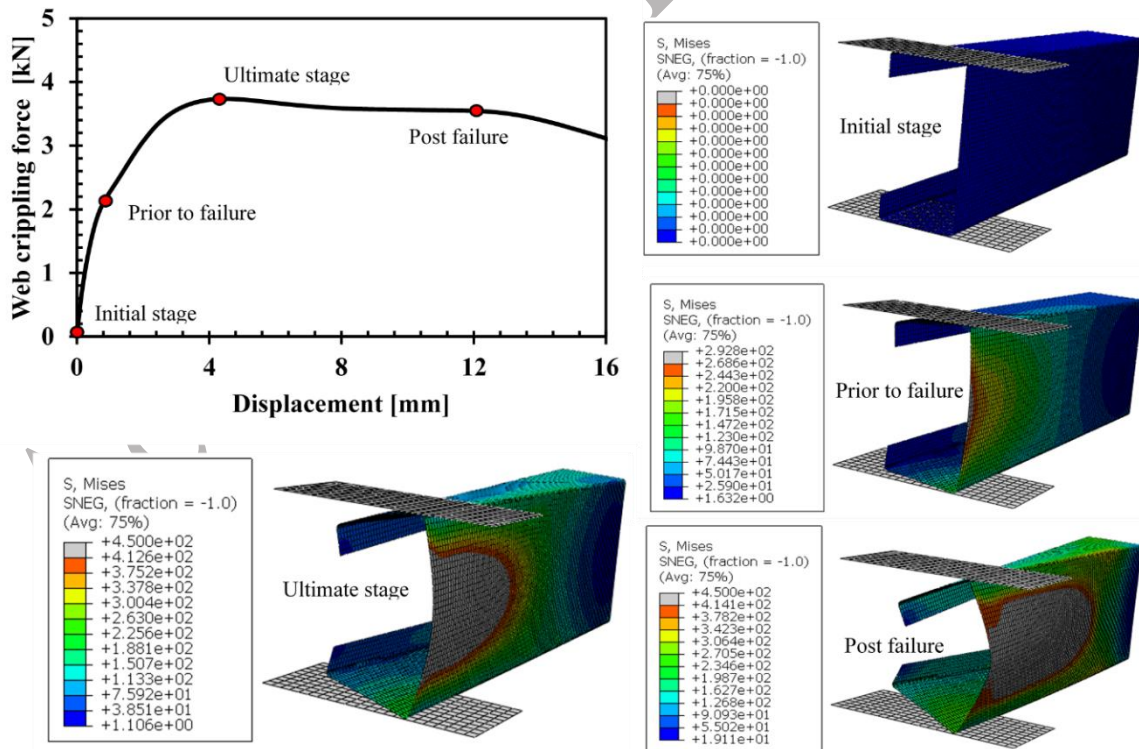
Fig. 13 Bending failure mode progression of optimised lipped channel beam for bending

Structures



478

Fig. 14 Shear failure mode progression of optimised lipped channel beam for shear



479

Fig. 15 Web crippling failure mode progression of optimised lipped channel beam for web crippling

480

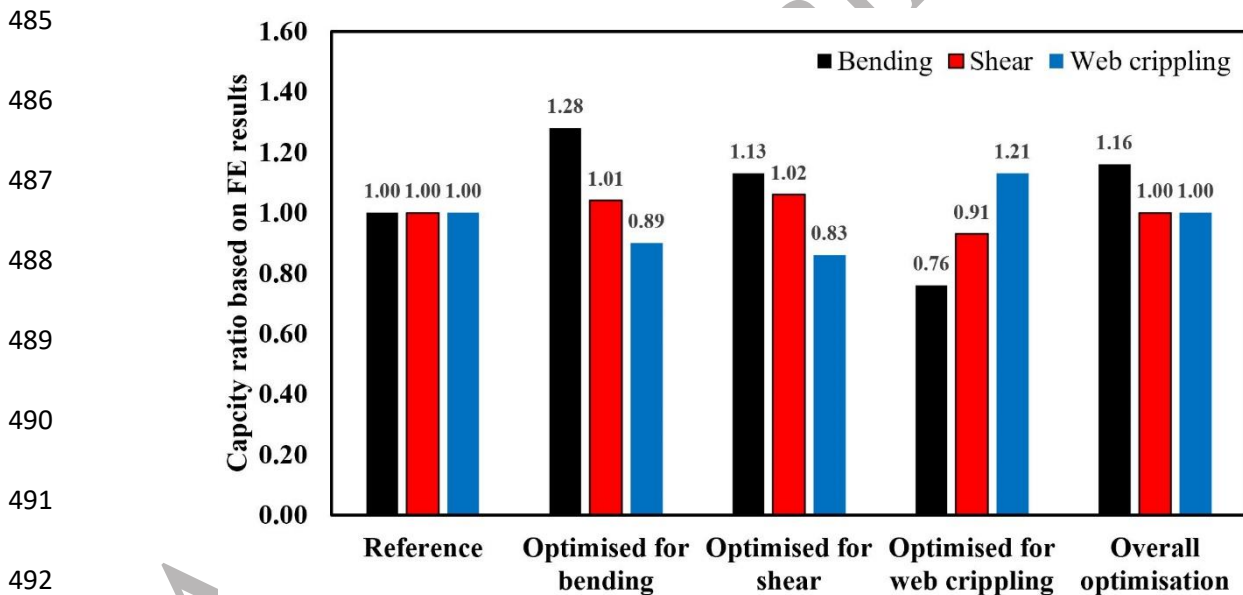
481

Structures

482 Table 6: Comparison of the bending, shear, and web crippling capacities of optimised lipped channel beams
 483 obtained from Eurocode3 (EC3) and FE analysis.

Optimisation criteria	Optimised capacities and other capacities (Eurocode 3)			Optimised capacities and other capacities (FE analysis)			EC3 /FE		
	$M_{c,Rd}$ (kNm)	$V_{b,Rd}$ (kN)	$R_{w,Rd}$ (kN)	$M_{c,Rd}$ (kNm)	$V_{b,Rd}$ (kN)	$R_{w,Rd}$ (kN)	M_{EC3}/M_{FE}	V_{EC3}/V_{FE}	R_{EC3}/R_{FE}
Reference (Fig. 5)	10.30	47.92	4.16	10.41	53.70	3.09	0.99	0.89	1.35
Bending (Eq. 10)	13.38	49.96	3.75	13.28	54.32	2.76	1.01	0.92	1.36
Shear (Eq. 11)	12.51	50.63	3.59	11.76	54.97	2.56	1.06	0.92	1.40
Web crippling (Eq. 12)	8.62	44.33	4.68	7.95	48.80	3.74	1.08	0.91	1.25
Combined (Eq.13)	11.59	47.92	4.16	12.08	53.70	3.09	0.96	0.89	1.34
Mean							1.02	0.91	1.34
COV							0.055	0.014	0.047

484 Note: $M_{c,Rd}$ = Section moment capacity, $V_{b,Rd}$ = Shear resistance, $R_{w,Rd}$ = Web crippling strength.



493 **Fig. 16** Performance of the optimised lipped channel beams based on FE results

494 5 Discussion of results

495 Several observations were made while performing the optimisation process for bending, shear,
 496 web crippling, and combined actions. The optimisation for bending resulted in a relatively
 497 slender section of lipped channel beam and showed approximately a 30 % enhancement in the
 498 bending capacity over the same amount of material used. The optimised dimensions for
 499 bending also resulted in shear capacity enhancement of 4 % and web crippling strength

Structures

500 reduction of 10% compared to reference lipped channel section. Optimising the dimensions
501 intend to maximise the shear capacity registered only 6 % of the shear resisting capacity
502 enhancement. In addition, the optimisation for shear reduces the web crippling capacity by
503 14% and enhancement in bending capacity by 21% compared to the reference lipped channel
504 beam. Optimisation for web crippling resulted in 13 % of the web crippling capacity
505 enhancement compared to the reference lipped channel beam. However, the performance of
506 under bending and shear actions is relatively poor with 16% and 7 % reduction, respectively.

507 The overall optimisation strategy appeared to be acceptable, as it showed reasonable results
508 without any reduction of the bending, shear, and web crippling capacities compared to
509 reference lipped channel beam. The shear and web crippling capacities remained similar as the
510 reference lipped channel beam, thus there was not any alteration in the dimension of the web
511 compared to the reference section. This can be argued that shear capacity increases with web
512 depth while web crippling capacity reduces with web depth. To satisfy both shear and web
513 crippling, the optimisation resulted in similar dimensions for the web as a reference section.
514 However, the flange and lipped dimensions varied themselves during the combined
515 optimisation such that the lip reached the upper bound and the flange attained the remaining
516 material thus maximising the second moment of area. However, the bending capacity
517 enhancement was 12%, compared to reference lipped channel beam.

518 The accuracy of the optimisation results was examined by developing FE models. The
519 developed FE models showed excellent agreement with the experiment results. The section
520 moment capacities obtained from FE analyses showed satisfactory agreement with the
521 capacities obtained using Eurocode 3 [18, 19] for the optimised sections. The EN1993-1-5
522 [19] shear predictions are, however, relatively conservative compared to FE results as EN1993-
523 1-5 [19] does not consider the enhanced value of shear buckling coefficient due to the
524 additional fixity in web-flange juncture as proposed in [5]. It is important to note that unsafe
525 predictions for web crippling capacities were observed from EN1993-1-3 [18] compared to
526 the FE results. Sundararajah et al. [4] have also acknowledged that EN1993-1-3 [18] prediction
527 for web crippling strength under ETF and ITF load case are either over-conservative or unsafe.
528 Therefore, shear and web crippling calculations appear in Eurocode 3 [18, 19] need an update.

529 It is finally proposed that based on the results obtained in this study the combined optimisation
530 criteria suits well with ~12 % bending capacity increase without compromising the shear and
531 web crippling capacities. Optimisation for bending criteria also suits well with enhancements
532 in bending and shear capacities and only 10% reduction in web crippling capacity.

Structures

533 6 Conclusions

534 In this paper, the CFS lipped channel beam was optimised for combined bending, shear, web
535 crippling using PSO algorithm. The ultimate capacity and structural behaviour of the optimised
536 lipped channels also simulated using validated FE models. Based on the findings following
537 conclusions can be drawn.

- 538 • The individual optimisation for bending, shear, and web crippling actions resulted
539 in 30 %, 6 %, and 13 % of capacity increase, respectively compared to the reference
540 section with the same amount of material.
- 541 • The newly proposed concept of combined optimisation resulted in the ~12 %
542 bending capacity increase without compromising the shear and web crippling
543 capacities.
- 544 • It is concluded that individual optimisation for bending and combined optimisation
545 will both result in efficient lipped channel CFS beams.
- 546 • FE models predicted satisfactorily the section moment capacities of the optimised
547 sections. Eurocode 3 calculations for shear and web crippling are conservative and
548 unsafe, respectively compared to FE predictions.
- 549 • The combined performance of bending, shear, and web crippling can be enhanced
550 using the proposed novel optimisation concept.

551 *Acknowledgements*

552 The authors would like to thank Northumbria University for financial support and providing
553 necessary research facilities to conduct this research project.

554 **References**

- 555 [1] C.H. Pham, G.J. Hancock, Experimental Investigation and Direct Strength Design of High-
556 Strength, Complex C-Sections in Pure Bending, *Journal of Structural Engineering* 139(11) (2013)
557 1842-1852.
- 558 [2] C. Yu, B.W. Schafer, Distortional buckling test on cold-formed steel beams, *Journal of Structural*
559 *Fire Engineering* 132(4) (2006) 515-528.
- 560 [3] R. Siahaan, M. Mahendran, P. Keerthan, Section moment capacity tests of rivet fastened
561 rectangular hollow flange channel beams, *Journal of Constructional Steel Research* 125 (2016) 252-
562 262.
- 563 [4] L. Sundararajah, M. Mahendran, P. Keerthan, Experimental Studies of Lipped Channel Beams
564 Subject to Web Crippling under Two-Flange Load Cases, *Journal of Structural Engineering* 142(9)
565 (2016).
- 566 [5] P. Keerthan, M. Mahendran, Experimental investigation and design of lipped channel beams in
567 shear, *Thin-Walled Structures* 86 (2015) 174-184.

Structures

- 568 [6] C.H. Pham, G.J. Hancock, Numerical simulation of high strength cold-formed purlins in combined
569 bending and shear, *Journal of Constructional Steel Research* 66(10) (2010) 1205-1217.
- 570 [7] W.-X. Ren, S.-E. Fang, B. Young, Analysis and design of cold-formed steel channels subjected to
571 combined bending and web crippling, *Thin-Walled Structures* 44(3) (2006) 314-320.
- 572 [8] L. Sundararajah, M. Mahendran, P. Keerthan, New design rules for lipped channel beams subject
573 to web crippling under two-flange load cases, *Thin-Walled Structures* 119 (2017) 421-437.
- 574 [9] P. Keerthan, M. Mahendran, Numerical Modeling of LiteSteel Beams Subject to Shear, *Journal of*
575 *Structural Engineering* 137(12) (2011) 1428-1439.
- 576 [10] M.R. Haidarali, D.A. Nethercot, Finite element modelling of cold-formed steel beams under local
577 buckling or combined local/distortional buckling, *Thin-Walled Structures* 49(12) (2011) 1554-1562.
- 578 [11] K. Roy, H.H. Lau, T.C.H. Ting, B. Chen, J.B.P. Lim, Flexural capacity of gapped built-up cold-
579 formed steel channel sections including web stiffeners, *Journal of Constructional Steel Research* 172
580 (2020).
- 581 [12] A. Uzzaman, J.B.P. Lim, D. Nash, K. Roy, Cold-formed steel channel sections under end-two-
582 flange loading condition: Design for edge-stiffened holes, unstiffened holes and plain webs, *Thin-*
583 *Walled Structures* 147 (2020).
- 584 [13] J. Ye, I. Hajirasouliha, J. Becque, K. Pilakoutas, Development of more efficient cold-formed
585 steel channel sections in bending, *Thin-Walled Structures* 101 (2016) 1-13.
- 586 [14] J. Ye, I. Hajirasouliha, J. Becque, A. Eslami, Optimum design of cold-formed steel beams using
587 Particle Swarm Optimisation method, *Journal of Constructional Steel Research* 122 (2016) 80-93.
- 588 [15] G. Perampalam, K. Poologanathan, S. Gunalan, J. Ye, B. Nagaratnam, Optimum Design of Cold-
589 formed Steel Beams: Particle Swarm Optimisation and Numerical Analysis, *ce/papers* 3(3-4) (2019)
590 205-210.
- 591 [16] P. Gatheeshgar, K. Poologanathan, S. Gunalan, B. Nagaratnam, K.D. Tsavdaridis, J. Ye,
592 Structural behaviour of optimized cold-formed steel beams, *Steel Construction* (2020).
- 593 [17] P. Gatheeshgar, P. Keerthan, G. Shanmuganathan, T. Konstantinos Daniel, N. Brabha, I. Eleni,
594 Optimised cold-formed steel beams in modular building applications, *Journal of Building Engineering*
595 (In press) (2020).
- 596 [18] CEN, Eurocode 3 - Design of steel structures - Part 1-3 General rules- Supplementary rules for
597 cold-formed members and sheeting, European Committee for Standardization, Brussels, 2006.
- 598 [19] CEN, Eurocode 3 - Design of steel structures - Part 1-5, Plated structural elements, European
599 Committee for Standardization Brussels, 2006.
- 600 [20] D.M.M.P. Dissanayake, K. Poologanathan, S. Gunalan, K.D. Tsavdaridis, B. Nagaratnam, K.S.
601 Wanniarachchi, Numerical modelling and shear design rules of stainless steel lipped channel sections,
602 *Journal of Constructional Steel Research* (2019).
- 603 [21] J. Lee, S.-M. Kim, H.-S. Park, B.-H. Woo, Optimum design of cold-formed steel channel beams
604 using micro Genetic Algorithm, *Engineering Structures* 27(1) (2005) 17-24.
- 605 [22] ABAQUS, Hibbit, Karlsson & Sorensen, Inc., Paw-tucket, USA, 2017.
- 606 [23] B.W. Schafer, T. Pekoz, Computational modeling of cold-formed steel: characterizing geometric
607 imperfections and residual stresses, *Journal of Constructional Steel Research* 47 (1998) 193-210.
- 608 [24] R. Siahaan, P. Keerthan, M. Mahendran, Finite element modeling of rivet fastened rectangular
609 hollow flange channel beams subject to local buckling, *Engineering Structures* 126 (2016) 311-327.
- 610 [25] P. Keerthan, M. Mahendran, New design rules for the shear strength of LiteSteel beams, *Journal*
611 *of Constructional Steel Research* 67(6) (2011) 1050-1063.
- 612 [26] B.W. Schafer, Z. Li, C.D. Moen, Computational modeling of cold-formed steel, *Thin-Walled*
613 *Structures* 48(10-11) (2010) 752-762.
- 614 [27] N. Degtyareva, P. Gatheeshgar, K. Poologanathan, S. Gunalan, M. Lawson, P. Sunday,
615 Combined bending and shear behaviour of slotted perforated steel channels: Numerical studies,
616 *Journal of Constructional Steel Research* 161 (2019) 369-384.
- 617 [28] P. Keerthan, M. Mahendran, D. Hughes, Numerical studies and design of hollow flange channel
618 beams subject to combined bending and shear actions, *Engineering Structures* 75 (2014) 197-212.

619